PROCEEDINGS OF SPIE

SPIEDigitalLibrary.org/conference-proceedings-of-spie

Miniature laser Doppler anemometers using solid state laser diodes

Christopher McLean
Cengiz Camci

SPIE.

Miniature Laser Doppler Anemometers Using Solid State Laser Diodes

Chris McLean and Cengiz Camci

The Pennsylvania State University, Department of Aerospace Engineering
Turbomachinery Heat Transfer Lab
233 Hammond Building, University Park, PA 16802

ABSTRACT

A single component continuous wave (CW) heterodyne laser Doppler anemometer (LDA) was constructed based on solid state technology for use in fluid dynamic research. The system design was motivated by the need for a miniature system capable of withstanding harsh operating environments. Such environments are often unavoidable when measuring high temperature combustion flows and when performing measurements in the field. With the recent advancements in solid state laser diodes and solid state avalanche photo diodes (APD), it is possible to construct miniature laser Doppler anemometers employing only solid state technology. Such systems have the advantages of small size, light weight, low power consumption, low cost, and ruggedness. The subject of the current research was to evaluate a visible laser diode's abilities and limitations in such a miniaturized LDA system.

A basic one dimensional LDA was designed, constructed and thoroughly tested employing a 10 milliwatt visible (670 nm) laser diode. The problems specifically associated with the use of a laser diode as a source are discussed, and their solutions presented. Data for the LDA evaluation measurements in a free jet facility is presented, and the results are compared to measurements obtained by hot-wire and five-hole probes. The miniature solid state LDA system was to found to possess accuracies of 2% for mean velocities and accuracies of 5-20% for RMS turbulent velocities.

Overall, the miniature LDA system with the solid state laser diode was found to be capable of accurate fluid dynamic measurements, and it appears to hold promise in enabling LDA measurements in before impractical situations.

1. INTRODUCTION

1.1 General statement of the problem

The heterodyne laser Doppler anemometer (LDA) has become an established flow measurement device in experimental fluid dynamics research. Theoretically, laser Doppler anemometers are capable of very impressive measurements making them attractive measurement tools. As with any measurement system however, there are very distinct advantages and disadvantages. Table 1.1 lists eight of the major advantages for using a laser Doppler anemometer.

TABLE 1.1
Heterodyne Laser Doppler Anemometer Advantages

- No Calibration Necessary
- Linear Velocity Response
- Can Measure Reversing Flows with Modifications
- Three-Component Simultaneous Measurements are Possible
- Non-Intrusive
- Well Defined Directional Response
- High Spacial and Temporal Accuracy
- High Frequency Response

0-8194-1091-8/93/$6.00

There are many complications which arise due to traditional LDA design and construction. For most cases, the problems can be overcome if some inconvenience or loss of accuracy may be tolerated. Apart from signal processing and seeding problems, table 1.2 lists several complications associated with traditional heterodyne laser Doppler anemometers. As can be seen from Table 1.2, many of the problems associated with standard LDA use can be linked to size and fragility.

TABLE 1.2
Heterodyne Laser Doppler Anemometer Complications

- Comprised of delicate instruments (~1 Watt Argon-Ion laser, Photo Multiplier Tubes)
- Lasers need large quantities of electrical power and cooling water
- Optical access problems
- High cost of investment (~ $200k)
- Large heavy construction makes traversing cumbersome
- Measuring seed velocity not flow velocity

Advances have been both proposed and marketed that can minimize some of the aforementioned complications. Following the advances of single-mode and multi-mode fiber optics, successful fiber head LDA systems have been realized. These systems are now widely available and seem to be the LDA user's choice for the future. However, even these miniature fiber head LDA systems have their drawbacks. While they eliminate much of the effective size, and weight associated with LDA use, fiber head LDA systems still require a remote optically connected Argon-Ion laser and receiving optics. This optical connection requires that the laser and photomultipliers be relatively close to the probe head. Such a limitation is not practical for many measuring environments such as when high vibrations are present or when moving frames of reference are involved. Passing the laser beams from a stationary frame to a moving or rotating frame is not easily achieved with fiber optics. What is needed for many situations is a completely optically isolated (electrical connections only) miniature laser Doppler anemometer which is both accurate and rugged.

In recent years (circa 1980's) much progress has been made towards developing a complete stand-alone miniature laser Doppler anemometer (Bopp et al. [1988], Damp [1988], Durst et al. [1991]). Such early systems were realized by employing both solid state laser diodes and solid state avalanche photodiodes along with simplified optical arrangements. These solid state based laser Doppler anemometers have several distinct advantages over both traditional and fiber optic LDA systems. Table 1.3 lists the advantages of using a miniature solid state LDA.

TABLE 1.3
Miniature Solid State Laser Doppler Anemometer Advantages

- Small Size - Easily comparable to optical fiber probe heads (tennis ball can size)
- Light Weight - Hand manipulatable
- Extremely Rugged - Entire solid state construction with no tubes
- Relatively Inexpensive - No large tables, traversers, or complex lasers
- Connected Only Electrically - No cooling waters, or optical fibers
- Minimal Power Consumption - Battery operated laser diode

There are many novel uses awaiting miniature solid state laser Doppler anemometers. Miniature systems enable fluid flow measurements in traditionally impossible or impractical configurations. Obvious candidates for such implementation would include flow measurements with optical access problems or stringent traversing requirements. However, these measurements could just as easily be accomplished with existing fiber optic LDA systems. Other less obvious candidates (but more exciting) for implementation include measurement environments with high vibrations, measurements in the field with portable systems, as well as measurements in machinery with rotating or moving frames of reference.

Measuring velocities directly in a rotating or moving frame of reference is not currently practical even with a miniature optical fiber head LDA due to the need for optical connections and large power requirements. No such requirements are necessary for solid state miniature LDA systems which only require electrical connections. Miniature solid state LDA systems could take turbomachinery rotor measurements directly in the rotating frame of reference. Such capability would enable highly resolved boundary layer studies to be undertaken in rotating machinery. Measurements about a moving vehicle could also be accomplished

rather easily. Measuring the flow field about a moving automobile or aeroplane while in motion would be no more difficult than taking stationary wind tunnel data.

Truly, there exist many interesting uses for miniature solid state laser Doppler anemometers. Due to the promise of measurement capabilities previously only dreamed of, there have been numerous attempts to build such miniature systems. Many problems have been uncovered, but much still remains to be learned. Additional research will be needed to clarify and quantify the problems associated with this promising new measurement device.

1.2 Specific research objective

It was decided to construct a single component heterodyne continuous wave laser diode based LDA for use in a quantitative evaluation. After evaluating prior work, it was noted that while many laser diode based LDA systems had been constructed (Bopp et al. [1988], Damp [1988], Durst et al. [1991]), no exhaustive evaluation of such a system had been performed. Previous works were typically concerned with proof of concept rather then the development of an accurate measurement tool. Consequently, it was decided that a detailed evaluation of laser diode LDA would be very beneficial in determining the usefulness of a laser diode based LDA for fluid dynamic measurements. Essentially, could a laser diode be used to generate accurate LDA data (both mean and turbulence quantities) in a real fluid flow? The end result of the evaluation process was to develop an LDA system comparable in accuracy to traditional systems.

1.3 General heterodyne LDA theory

Most modern laser Doppler systems used in fluid dynamic research are heterodyne systems. A simple one-dimensional heterodyne system is shown in figure 1. For the purposes of explanation the LDA fringe model will be used. The analysis could be equally performed using the Doppler model resulting in identical results for the case at hand.

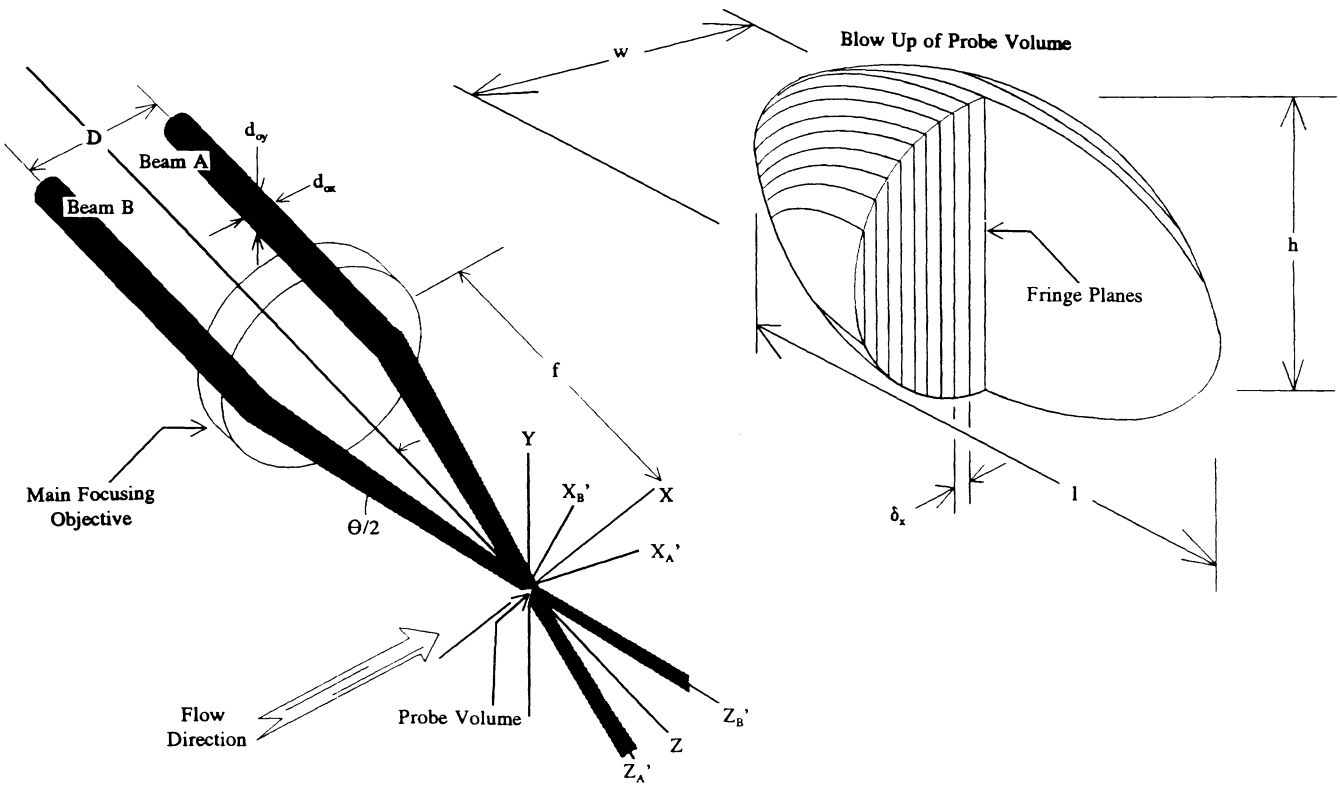

FIGURE 1
Simple One-Dimensional Heterodyne LDA Geometry

The underlying theory behind the laser Doppler anemometer is quite simple. A coherent polarized laser beam is split equally into two beams and then the beams are brought to cross at a focal point (*probe volume*). In the probe volume, interference fringes exist (if a surface is present) due to interference between the phase fronts of the two propagating coherent beams which are typically assumed flat in the focal region. The distance between two interference maxima is given by equation 1.

$$\delta_x = \frac{\lambda}{2 \sin\frac{\Theta}{2}} \tag{1}$$

As small seed particles (typically $\approx$ 1-10 μm) carried by the flow pass through the probe volume, laser light is scattered. The intensity of the scattered light is dependent on the amount of interference taking place at the location where the particle is, and on the particles diameter. The scattered light is collected and focused onto a square-law photodetector, and an intensity fluctuation in time is observed with a frequency related to the velocity of the fluid particle through the fringes. This frequency is referred to as the *Doppler frequency* and it is directly related to the velocity component in the x-direction, the laser wavelength, and the half angle. The Doppler frequency is given by equation 2.

$$F_d = \frac{2U_x}{\lambda} \sin(\frac{\Theta}{2}) \tag{2}$$

It should be noted that the Doppler frequency is a function of a single velocity component. This situation proves useful in constructing simultaneous multi-component measurement systems from multiple single systems.

The edge of the probe volume is defined to be where the intensity difference between an interference maxima and minima falls to $1/e^2$ of this difference at the probe volume center. Many factors will effect the effective probe volume shape such as processing criteria, collection location, and particle size. Using an optical field model for a Gaussian laser beam the ideal probe volume extents can be found to be an ellipsoid. Assuming that the half angle is small, neglecting wavefront curvature, and assuming that the diameters of the laser beams do not vary over the probe volume, the dimensions of the probe volume are given by equations 3 through 5.

$$l = \frac{4\lambda f}{\pi d_o \sin\frac{\Theta}{2}} \tag{3}$$

$$w = \frac{4\lambda f}{\pi d_o} \tag{4}$$

$$h = \frac{4\lambda f}{\pi d_o} \tag{5}$$

where $d_0 = d_{0x} = d_{0y}$ for circular Gaussian beams. A typical ellipsoidal probe volume is shown in figure 2.

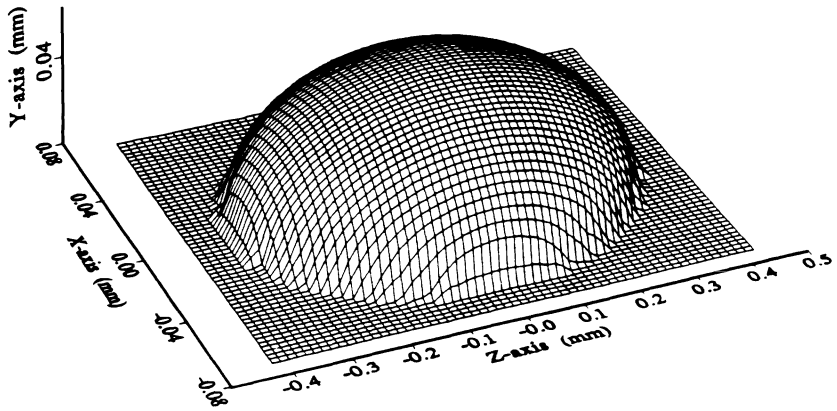

FIGURE 2
Top Half of Ellipsoidal Probe Volume for Circular Gaussian Laser Beams

2. MINIATURE LASER DIODE HETERODYNE LDA SYSTEM

2.1 LDA design concerns

Before any hardware was purchased or assembled, the general guiding parameters for the miniature laser Doppler system were set forth. The accuracy of the instrument would be produced by using high quality components, but only where essential due to cost constraints. Table 2.1 lists the guiding design parameters used. It should be kept in mind that the device was being designed for fluid dynamic measurement situations involving harsh environments.

TABLE 2.1
Guiding Design Parameters

Parameter	Quantity and Rational
• Collection	Backscatter for maximum flexibility of access
• Measuring Components	One for simplicity, and due to limited wavelength availability
• Size	Under 100 × 100 × 300 mm for handling and traversing ease
• Weight	Under 3 kg for handling and traversing ease
• Durability	Withstand 500 g acceleration for high durability
• Power	Run laser for 24 hrs on small batteries for portability
• Cost	Under $7500.00 *including* visible laser diode, collimating optics, circularizing optics, beam splitter, focusing/receiving optics, and avalanche photodiode. *Excluding* signal processing equipment
• Accuracy	Mean to 1% and turbulence to 5% for fluid dynamics research

The design and construction of the miniature laser Doppler anemometer was far from elementary. It involved attempting to meet the general guidelines set forth above while working to overcome the laser diode's inherent problems and limitations. In the end, a balance between the systems complexity and accuracy needed to be achieved. Additional complexity would improve the accuracy of the LDA, but the penalties would be increased size, weight, fragility, and expense which could not be tolerated.

Following several design iterations, an accurate working miniature LDA system was fashioned. The choice of the laser diode was the most important of all of the components. A poor quality laser diode would destroy any chances of accuracy regardless of the amount of added optical correction procedures. It was decided for this reason to sacrifice the cost guideline for this component. The high quality solid state laser diode would allow for simpler (less expensive) correction optics to be used which would improve the overall design. For use in the miniature LDA system, the laser diode needed to possess some very specific traits. First, the solid state laser needed to draw no more than 100 mA of current so that it could be powered by 4 AA batteries over a 24 hour period. Second, a visible wavelength was desired to allow for ease of alignment and adjustment. Third, if clean fringes were to be produced in the probe volume the laser needed to have a high polarization ratio, low astigmatism, and high coherence. And lastly, for stability the wavelength temperature drift needed to be very low.

2.2 Final constructed miniature LDA

A suitable laser diode was found which had the qualities necessary for use in a heterodyne LDA. The laser diode was combined with other essential optical components (collimator, circularizer, splitter, lenses, photodiode, etc.) to form the miniature laser diode based LDA. The specifications of the miniature system are given in table 2.2, and a schematic of the complete LDA system is given in figure 3. The system was assembled on an optical breadboard for ease in alignment and adjusting.

TABLE 2.2
Specifications of the Miniature
Laser Diode Based Laser Doppler Anemometer

Specification	Quantity
• Diode Style	Index Guided
• Diode Wavelength	670 nm (visible red)
• Diode Optical Power	9.9 mW
• Diode Astigmatism	11 μm
• Diode Polarization Ratio	400:1
• Diode Lasing Mode	Single Spatial and Temporal
• Diode Coherence Length	~5 mm
• Diode Linewidth	6.0×10^4 MHz (or 0.09 nm)
• Diode Current Drain	70 mA
• Diode Temperature Drift	0.25 nm/°C (including mode hoping effects)
• Diode Beam Divergence	~11° × ~40°
• Size (L × H × W)	270 × 100 × 200 mm
• Main Objective Focal Length	150 mm
• Half Angle (Θ/2)	9.939°
• Probe Volume Length	0.741 mm
• Probe Volume Width	0.128 mm
• Probe Volume Height	0.128 mm
• Fringe Separation	1.94 μm
• Number of Fringes	66
• Velocimeter Transfer Constant	~0.49 MHz/(m/s)

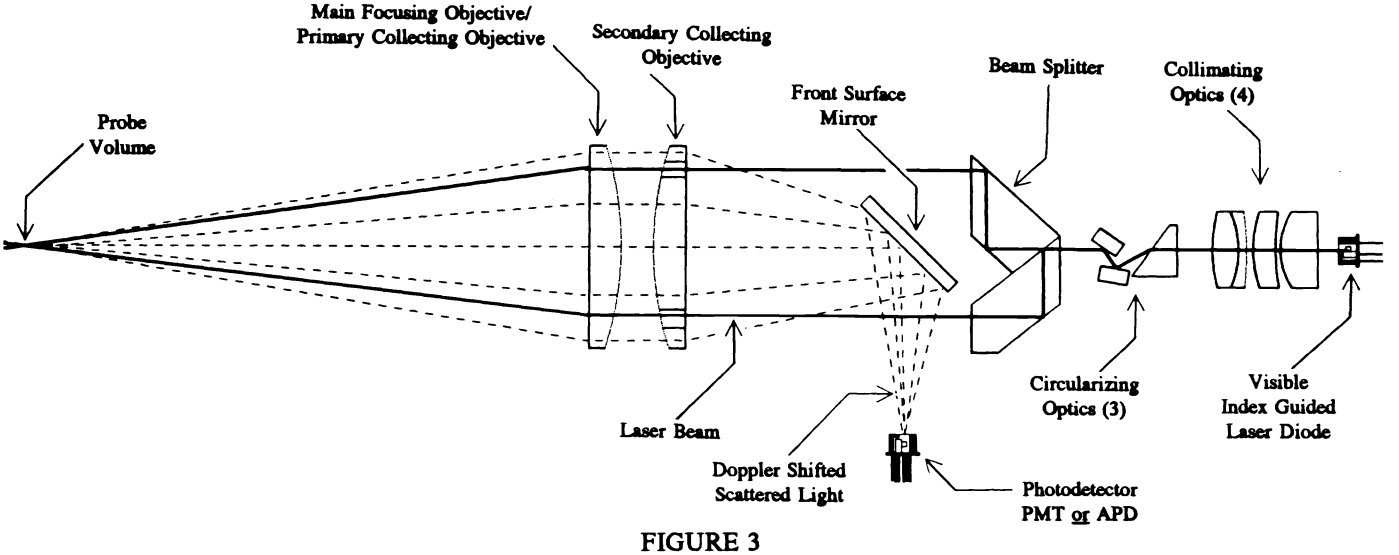

FIGURE 3
The Miniature LDA System Schematic (Not To Scale)

3. CONSEQUENCES OF USING LASER DIODES IN HETERODYNE LDA

3.1 Solid state laser use in an LDA system

A typical laser diode beam is characterized with many traits which make its use in LDA systems questionable. However, with proper optical correction techniques, solid state lasers can be successfully used in miniature heterodyne LDA systems. Figure

4 shows an index guided laser diode, and table 3.1 states the beam characteristics attainable from a quality index guided solid state laser.

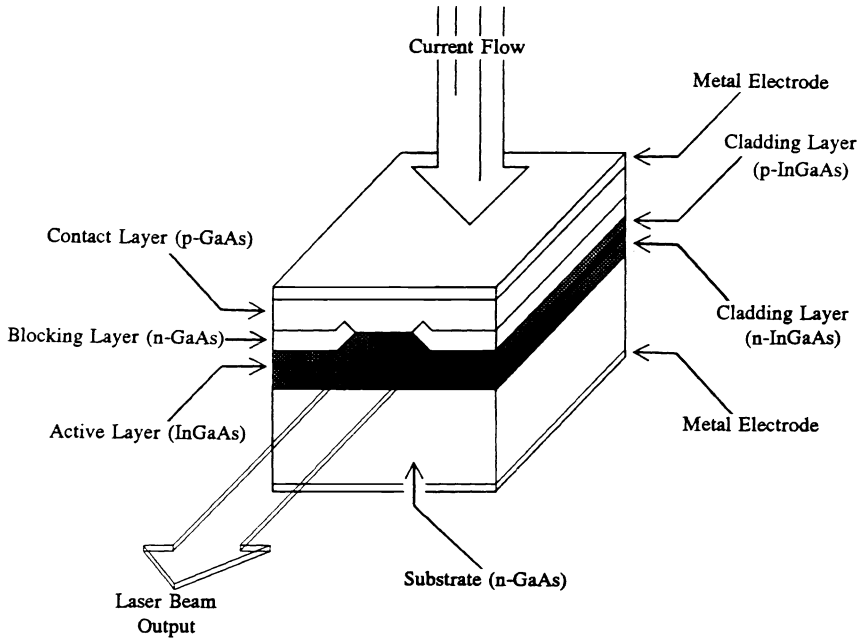

FIGURE 4
Index Guided Laser Diode

TABLE 3.1
Index Guided Laser Diode Characteristics As related to LDA Use

Laser Beam Field Distribution:
- Similar operational mode to TEM_{00}
- Gaussian intensity profile in the parallel transverse direction
- Lorentzian intensity profile in the perpendicular transverse direction
- Differing high divergences in parallel and perpendicular transverse directions
- Elliptical diverging beam in the far field

Laser Beam Power:
- High optical output power to size ratio
- Low optical power of 5-10 mW

Laser Beam Wavelength:
- Visible and infrared wavelengths available
- Multiple simultaneous operating wavelengths over several nanometers possible due to wide gain range
- Low coherence length due to high rate of spontanious emissions
- Wavelength sensitive to junction temperature, current density, and reflections into cavity

Laser Beam Optical Parameters:
- High astigmatism due to different apparent emission locations of perpendicular and parallel profiles
- High polarization ratio possible of ~400:1

The use of a solid state laser allows the miniaturization of LDA transmission systems, but with the expectation of degraded performance. Crucial areas that require consideration are low power, high divergence, elliptical beam, multiple simultaneously emitted modes, low coherence, and wavelength drift. Only with a properly selected laser diode and following multiple correctional measures can an accurate LDA system be achieved.

3.2 LDA probe volume with a diode laser beam

It was initially expected that there would be substantial differences between a standard LDA based on a circular Gaussian laser and one based on a diode laser. In an effort to discover any differences an optical analysis was performed to determine the probe volume characteristics.

The laser diode beam first needed to be optically modeled. It has been shown by Bopp et al. [1988] that for a collimated laser diode the normalized transverse optical field magnitudes may be adequately represented by equations 6 and 7 (Gaussian and Lorentzian distributions respectively).

$$E_y = e^{-(\frac{2y}{D_y})^2} \tag{6}$$

$$E_x = \frac{\xi D_x^2}{\xi D_x^2 + x^2} \tag{7}$$

Where ξ is given by

$$\xi = \frac{1}{4(e - 1)} \approx 0.1454941 \tag{8}$$

The electrical field distribution in the parallel transverse direction is given by E_x while the perpendicular transverse field distribution is given by E_y. Not only do the field distributions differ in the two transverse directions, but the beam diameters typically differ as well. The electrical field is separable so the complete field is found simply by multiplying the two transverse profiles. The resulting optical field magnitude may be represented by equation 9.

$$E(x,y) = [e^{\frac{-4y^2}{D_y^2}}] \, [\frac{\xi D_x^2}{\xi D_x^2 + x^2}] \tag{9}$$

For use in heterodyne LDA the laser diode beam is split into two beams (A & B) each having equal electrical field magnitudes then the beams are focused to a crossing point where the fringes may be said to exist. It is assumed that the two distributions for each of the beams focus to the same point. In general the point of crossing will not be at the lens' focal point, and the beam waist will not be at the point of crossing. However if one is careful in the beam collimation and focusing the beams can be made to focus at the same point. The diameter of the focused A beam near the focal point may be found from

$$D_{x'_A} = \sqrt{\frac{16\lambda^2 f^2}{\pi^2 d_{ox}^2} + \frac{d_{ox}^2 \, z'^2_A}{f^2}} \tag{10}$$

in the x'_A direction, and

$$D_{y_A} = \sqrt{\frac{16\lambda^2 f^2}{\pi^2 d_{oy}^2} + \frac{d_{oy}^2 \, z'^2_A}{f^2}} \tag{11}$$

in the y direction. Similar equations hold for the B beam replacing z'_A with z'_B.

The two focused crossing beams have field magnitude distributions with respect to their propagation axis (z'_A and z'_B respectively). The optical field magnitude of the A beam is now given by equation 12, and the optical field magnitude of the B beam is now given by equation 13.

$$E_A(x,y,z) = \frac{1}{2}[e^{\frac{-4y^2}{D_{y_A}^2}}]\,[\frac{\xi D_{x'_A}^2}{\xi D_{x'_A}^2 + x'^2_A}] \tag{12}$$

$$E_B(x,y,z) = \frac{1}{2}[e^{\frac{-4y^2}{D_{y_B}^2}}]\,[\frac{\xi D_{x'_B}^2}{\xi D_{x'_B}^2 + x'^2_B}] \tag{13}$$

where the transformations from the primed coordinates to the global coordinates are given by

$$x'_A = x\cos(\frac{\Theta}{2}) + z\sin(\frac{\Theta}{2}) \tag{14}$$

$$x'_B = x\cos(\frac{\Theta}{2}) - z\sin(\frac{\Theta}{2}) \tag{15}$$

$$z'_A = -x\sin(\frac{\Theta}{2}) + z\cos(\frac{\Theta}{2}) \tag{16}$$

$$z'_B = x\sin(\frac{\Theta}{2}) + z\cos(\frac{\Theta}{2}) \tag{17}$$

and the beam diameters are given by equations 10 and 11.

The two beams in the crossing region will interfere due to their wave nature. The beams can be said to have a magnitude (given by equations 12 and 13) and a phase. At locations where the two beams have equal phases the fields will combine to give a relative maximum, and at locations where the beams are completely out of phase the fields will subtract to give a relative minimum. At any spatial location in the probe volume either a maximum or a minimum may occur depending on such parameters as the wavelength and crossing geometry. For the purposes of this analytical study, the beams were assumed to possess infinite coherence lengths. In reality, the effect of the finite coherence length would tend to shrink the probe volume by degrading the interference of the two beams.

The probe volume extent is defined to be the location where the difference between an intensity maximum and an intensity minimum is equal to $1/e^2$ (i.e., fringe visibility = 0.13534) the value at the center of the crossing region. It should be kept in mind that the intensity is the square of the electric field magnitude. So, the intensity at a maximum is equal to

$$I_{max} = [E_A(x,y,z) + E_B(x,y,z)]^2 \tag{18}$$

and the intensity minimum is equal to

$$I_{min} = [E_A(x,y,z) - E_B(x,y,z)]^2 \tag{19}$$

The resultant fringe height is then given by the difference as stated in equation 20.

$$\Delta I = [E_A(x,y,z) + E_B(x,y,z)]^2 - [E_A(x,y,z) - E_B(x,y,z)]^2 \tag{20}$$

By setting equation 20 equal to $1/e^2$ the probe volume extent may be determined in terms of x, y and z.

The equation governing the probe volume is rather complex in nature. In order to resolve the shape a computer algorithm was developed to itteratively determine coordinate locations which satisfied equation 20. Input data for the various parameters were taken to be those of the current miniature LDA design:

- wavelength $\lambda = 670.0$ nm
- diameter in x $d_{ox} = 1.0$ mm
- diameter in y $d_{oy} = 1.0$ mm

- focal length $f = 150.0$ mm
- crossing angle $\Theta = 20.0°$

The resulting probe volume edge (fringe visibility = $1/e^2$) is displayed in figure 5.

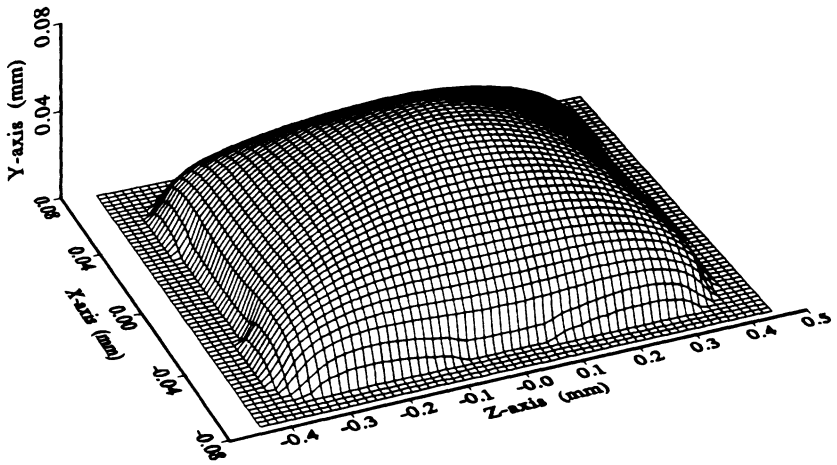

FIGURE 5
Top Half of Probe Volume Shape for Collimated Laser Diode Beams
Based on the $1/e^2$ Visibility Criteria

It is immediately apparent that there are differences between the laser diode probe volume and a typical Gaussian laser probe volume. The probe volume is no longer a simple ellipsoid. The general probe volume shape shown in figure 5 is typical for any realistic values of the input parameters including elliptical beams. The dimensions of the probe volume were found to be virtually identical to those generated by Gaussian lasers with the exception that the beam diameter is no longer unique but rather has two distinct values ($d_{ox} \neq d_{oy}$).

Although the probe volume dimensions are similar, the probe volume fringes will not be similar. The wavefront curvature associated with the Lorentzian profile is greater than the curvature associated with a Gaussian profile. Near the crossing point a Lorentzian beam does not reach the same level of flatness as a Gaussian beam would at the same location. Consequently, the effects of beam divergence are heightened. Beam divergence in the crossing region will cause interference fringe planes to have curvature. Essentially, the fringe spacing seen by particles traveling in the x direction varies in the Z and Y directions.

Deviations from this spacing can easily be as severe as +10% for Lorentzian beams (as opposed to roughly +1% for Gaussian). Accurate turbulence measurements are not possible with such high deviations. Actual fluid flow fluctuations (real turbulence) will be contaminated with fluctuations due to particle passing location (generating artificial turbulence).

In summary, the probe volume generated with a laser diode beam was found to have differences when compared to that generated with a Gaussian laser beam. The overall physical dimensions were found to be similar, but the shape of the probe volume was distorted. Fringe uniformity was expected to be significantly effected by the Lorentzian distribution's higher wavefront curvature in the crossing region.

4. EXPERIMENTAL EVALUATION

4.1 Experimental evaluation facility

With the miniature laser Doppler anemometer fully constructed and operational on an optical bread board, a quantification of the measurement uncertainty was required. A test flow was needed which would challenge the miniature LDA system. It was expected that the specific flow chosen would expose many of the LDA error sources thereby enabling a systematic evaluation of the system's performance under extreme conditions.

Velocity measurements in a stagnating round free jet were chosen for the purpose of quantitative evaluation. The flow would have several attributes which would require special attention for accurate LDA measurements. Namely, the flow possessed high velocity gradients, high local turbulence, large scale intermittency, and a large mean velocity range. Figure 6 displays a schematic of the test flow facility.

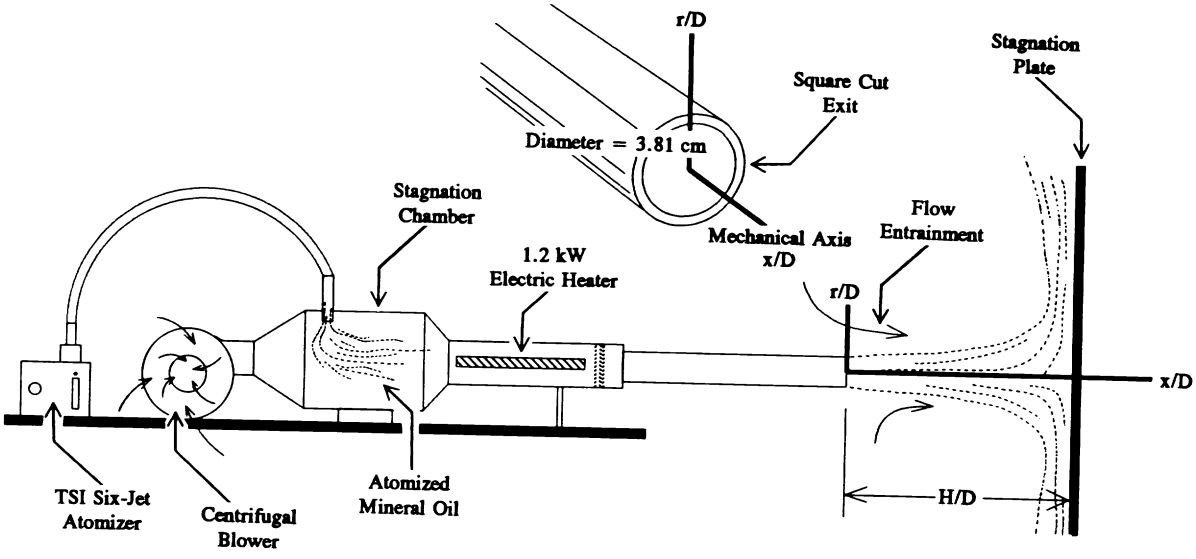

FIGURE 6
Experimental Test Flow Rig
(Heated Free Jet Facility)

Measurement surveys were performed at four x/D locations with three measurement devices: miniature LDA, five-hole probe and hot-wire probe. The five-hole and hot-wire probes are established measurement tools for the measurements of mean and turbulent velocities respectively. The LDA data was computed based on 2000 individual Doppler bursts (seed crossing probe volume occurrence) at each measurement point. Mineral oil of 1-3 μm diameter was generated with a six-jet atomizer and mixed with the air flow to be used as seed. The seeding density was set sufficiently low that only one or no particle would be in the probe volume at a time.

Velocity measurements for the LDA data were computed via a burst counter/processor and personal computer. The electronic processor appropriately filters the Doppler signal and determines the frequency by counting the time for a fixed number of cycles to be received. When operated properly, the processor is capable of highly accurate frequency determination (0.1%) at speeds of up to 10k bursts/s (seed crossing probe volume per second).

5. ERROR QUANTIFICATION AND ANALYSIS

5.1 General uncertainty analysis overview

The raw data measured with the laser diode based miniature laser Doppler anemometer was put through a rigorous error analysis. It was desired to both correct for quantifiable bias errors and to compute measurement uncertainties based on estimates for uncorrectable errors. The corrected mean velocity ($\bar{U}$) and RMS turbulent velocity (u_{RMS}) profiles with known uncertainties would then be compared to the hot-wire and five-hole data.

5.2 ASME standard uncertainty analysis

The adopted ASME standard measurement uncertainty methodology [Abernathy et al., 1985] was used exclusively in the analysis of the raw LDA data. The method provided a structured procedure for computing LDA measurement uncertainties based on the

precision and bias errors of numerous sources.

The uncertainty of any single measurement or parameter can be expressed in terms of precision errors and bias errors. The actual value of the measurement may be assumed to be the average of N measurements. The bias error (B_X) is the shift in the measurement average from the true value. Because the true value is never exactly known, it is difficult to assign accurate values to bias error terms. The precision error is related to scatter of the measurement data. A value known as the precision index (S_X) is used to quantify the precision error. Equation 21 defines the precision index.

$$S_X = \sqrt{\frac{\sum_{i=1}^{N} (X_i - \bar{X})^2}{N - 1}} \tag{21}$$

If a measurement is the result (via an equation) of several individual parameters (measurements), then a method is needed to compute the errors associated with that result. The errors in a particular result are directly related (through sensitivity factors) to the errors in the individual measurement parameters used to compute the result. A result such as

$$r = f\{P_i, P_{i+1}, P_{i+2}, \ldots, P_j\} \tag{22}$$

is a function of j parameters, and the sensitivity factors are simply the derivatives of the result with respect to the parameters. Namely,

$$\theta_{P_i} = \frac{\partial r}{\partial P_i} \tag{23}$$

Each of the j measurement parameters will in general have a precision index (S_{Pi}) and a bias error (B_{Pi}) associated with it. The precision and bias errors in the result (S_r and B_r) due to the precision and bias in the parameters (S_{Pi} and B_{Pi}) is given by equations 24 and 25.

$$S_r = \sqrt{\sum_{i=1}^{j} (\theta_{P_i} S_{P_i})^2} \tag{24}$$

$$B_r = \sqrt{\sum_{i=1}^{j} (\theta_{P_i} B_{P_i})^2} \tag{25}$$

Certain special instances apply when computing precision indices and bias errors in results. Two such situations will be addressed. First the uncertainty in a mean measurement, and second the uncertainty in an RMS measurement.

If the parameters (which are results themselves) are used with other similarly computed parameters to compute a mean parameter (such as $\bar{U}$ from u_i, u_{i+1}, u_{i+3}, etc.), then the precision index and bias error in the mean value are given by

$$S_{\bar{X}} = \frac{t S_{X_i}}{\sqrt{N}} \tag{26}$$

$$B_{\bar{X}} = B_{X_i} \tag{27}$$

where N is the number of times the parameter X_i was independently determined and t is the student t value ($t \approx 2$ for $N \geq 3$). The averaging process used to compute the result will tend to minimize the precision error (data scatter), but the bias error will be unaffected.

The uncertainty in an RMS value (such as u_{RMS} from u_i, u_{i+1}, u_{i+2}, etc.) based on the precision and bias errors of individual measurements is the second special case to be investigated. The precision and bias errors in an RMS value are given by

$$S_{X_{RMS}} = \frac{t(X_{RMS})}{\sqrt{N}} \sqrt{\left[\frac{S_{X_i}}{X_{RMS}}\right]^2 + \left[\frac{S_{\bar{X}}}{X_{RMS}}\right]^2} \tag{28}$$

$$B_{X_{RMS}} = 0.0 \tag{29}$$

The bias errors in individual measurements will have no effect on the uncertainty in the RMS value. Bias errors will only shift the measurement distribution, but the data scatter will remain unchanged. However, the precision errors in the individual

measurements will have a strong effect on the uncertainty in the RMS value.

While knowing the individual precision and bias errors in a measurement is often useful, often it is desirable to state a single quantity which characterizes the overall error in the result. The quantity of uncertainty is used for this purpose. The uncertainty in a result is taken to be a combination of both the precision and bias errors. For an uncertainty analogous to a 95% coverage, an RMS combination is used,

$$U_r = \sqrt{B_r^2 + S_r^2} \tag{30}$$

5.3 Miniature LDA uncertainty sources

There were many error sources investigated in the miniature LDA measurement uncertainty. Each of the error sources could potentially add both precision and bias errors to the computed mean velocity ($\bar{U}$) and the computed RMS turbulent velocity (u_{RMS}).

Six error sources leading to the measurement uncertainty of an individual velocity measurement were investigated for this research. An individual velocity measurement was calculated according to equation 31.

$$u_i = \frac{F_D \lambda}{2\sin(\frac{\Theta}{2})} \tag{31}$$

The velocity calculation is seen to be a function of three parameters; Doppler frequency (F_D), wavelength (λ), and the half angle ($\Theta/2$). Table 5.1 Lists the error sources, the affected parameter, and the type of error incurred by each. In addition seed biasing was investigated, but not quantified or included in the error analysis.

TABLE 5.1
Miniature LDA Uncertainty Error Sources
for Individual Doppler Burst Realization

Error Source (Effected Parameter)	Errors on Individual U Calculation
• Half Angle Measurement Uncertainty ($\Theta/2$)	Bias *only*
• Laser Diode Wavelength Uncertainty (λ)	Bias *only*
• Interference Plane Gradients Due to Misalignments (F_D)	Precision *only*
• Interference Plane Gradients Due to Lorentzian Intensity Distribution (F_D)	Precision and Bias
• Counter Comparison Criteria (F_D)	Precision *only*
• Counter Finite Clock Resolution (F_D)	Precision *only*
Error Source	**Errors on Velocity Distribution**
• High Velocity Biasing	Predominantly Mean Velocity Error
• Velocity Gradients Across the Probe Volume	Predominantly RMS Turbulence Error

Two styles of error sources are seen to exist. Those which act on individual parameters, and those which act on the entire distribution as a whole. The error sources acting on the distribution as a whole were corrected for through appropriate correction relations. In contrast, the parameter error sources are coupled so they may not be accurately corrected for. Instead the errors were propagated into the result to define a value of measurement uncertainty. The overall precision index and bias error in a single velocity measurement was computed as described previously by propagating the individual parameter errors into the instantaneous velocity result. Then the precision index and bias error for the 2000 individual velocity results were propagated again into the mean velocity and RMS turbulent velocity results. Following the double propagation procedure, an uncertainty value was assigned to the mean velocity and the RMS turbulence velocity through an RMS combination of the respective precision index and bias error. This procedure was repeated for every point in all 4 profiles.

Following the ASME uncertainty procedure outlined, the resultant precision index and bias error in a single velocity measurement were found to be given by

$$S_{u_i} = \sqrt{(\frac{\partial u_i}{\partial F_D} S_{F_D})^2 + (\frac{\partial u_i}{\partial \lambda} S_\lambda)^2 + (\frac{\partial u_i}{\partial \frac{\Theta}{2}} S_{\frac{\Theta}{2}})^2} \tag{32}$$

$$B_{u_i} = \sqrt{(\frac{\partial u_i}{\partial F_D} B_{F_D})^2 + (\frac{\partial u_i}{\partial \lambda} B_\lambda)^2 + (\frac{\partial u_i}{\partial \frac{\Theta}{2}} B_{\frac{\Theta}{2}})^2} \tag{33}$$

where the precision index for F_D is a combination of four precision indices as shown in equation 5.34.

$$S_{F_D} = \sqrt{(S_{F_{D1}})^2 + (S_{F_{D2}})^2 + (S_{F_{D3}})^2 + (S_{F_{D4}})^2} \tag{34}$$

5.3.1 Half angle measurement uncertainty

Due to the experimental method used for measuring the half angle, a bias error exists. Briefly, the two laser diode beam propagation vectors were determined with the aid of a pinhole and a precision 3-axis traverse. The angle between the two beams was then found by using the dot product relation between the two spatial vectors. The beam crossing angle should not change in time (neglecting laser beam walk) so every seed particle would see a probe volume defined by the same crossing angle. The current measurement capabilities allowed a bias error of 0.01° ($B_{\Theta/2} = 1.75 \times 10^{-4}$ rad) for the half angle measurement.

5.3.2 Laser diode wavelength uncertainty

The laser diode wavelength was not known exactly due to measurement capabilities resulting in a bias error. The wavelength emitted by the laser diode is a function of junction temperature, forward bias current, and reflected laser light. The laser diode was driven with a highly stable constant current source, and the LDA system used only high quality optics with antireflective coatings. However, the temperature of the junction was not actively controlled. Consequently, the laser diode wavelength was able to drift from the value measured at the beginning of the measurements to that at the end ($\sim$1 hour). It was assumed that the temperature remained constant during the 2000 Doppler bursts recorded for each point in the flow. This results in a bias error alone. The bias error (B_λ) was found to be 0.5 nm for temperature fluctuations of $\pm$2°C.

5.3.3 Interference plane gradients due to misalignments

Due to misalignments of the laser beam waist, the spacing between interference fringes may not be uniform throughout the probe volume causing a precision error. Hanson [1972] describes in detail the source of interference plane gradients. Essentially, a misplacement of the input beam waist causes a spatial difference between the beam crossing point and the location of minimum beam diameter. This spatial gap forces the probe volume to be formed by laser beams that are diverging. Such a situation causes the interference fringes to fan out having a different spacing at either end of the probe volume. The precision index (S_{FD1}) was computed to be $(1.69 \times 10^{-3})F_D$. The bias error from such a source is small and was neglected.

5.3.4 Interference plane gradients due to lorentzian distribution

Due to the Lorentzian intensity distribution in the plane of the beam crossing (x-z plane), the interference planes will be distorted additionally from those due to misalignments. The Lorentzian distribution error was discussed in detail by Durst et al. [1991]. The cause of the error stems from the high wavefront curvature and unevenness present with Lorentzian diode beams. Even for a properly aligned LDA system, the high wavefront curvature will cause the fringes to be curved. The fringe curvature becomes worse as the ends (along length) of the probe volume are approached, and this is augmented by the fact that the laser diode generated probe volume does not taper nearly as fast as a standard ellipsoidal probe volume. The size increase of the probe volume near the ends allows regions where high wavefront curvatures exists to fall within the Signal validation criteria. The double effect of larger probe volumes and increased wavefront curvature produces higher fringe curvatures than Gaussian beams would cause. The precision index (S_{FD2}) and bias error (B_{FD2}) were computed to be $(0.065)F_D$ and $(0.01)F_D$ respectively.

5.3.5 Signal processor comparison criteria and clock resolution

The signal processor due to its comparison criteria and its finite clock resolution was not able to report the Doppler frequency with zero uncertainty. Errors due to amplifier noise, improper filter settings, and false triggering were encompassed into the comparison error. The processor measures the Doppler frequency at two different times for the same Doppler burst and compares the two values then the measurement is rejected if they differ by more than the comparison criteria. Processing continues until 2000 valid bursts are recorded. Then the LDA system moves to the next measurement position. A comparison criteria of 1% was used for validating the processing of an individual Doppler burst, and the processor clock had a resolution of 1 nanosecond. For timing 8 cycles the two precision indices became $(0.01)F_D$ for the comparison criteria (S_{FD3}) and $(1.25\times10^{-10}s)F^2_D$ for the clock resolution (S_{FD4}).

5.4 Experimental results following corrections and uncertainty

The raw miniature LDA measurement results were put through the uncertainty procedure described thus far. The measurements were corrected for expected bias errors due to both high velocity biasing and finite spatial resolution biasing. Then uncertainties were determined for the corrected measurements based on errors in half angle measurement, laser diode wavelength uncertainty, interference plane gradients (due to misalignments and Lorentzian distribution), and signal processor resolution. Figure 7 displays measured profiles for x/D = 2 (midway between jet exit and stagnation plate) following bias corrections and uncertainty calculations. The errors determined through a comparison of the corrected miniature LDA data with the hot-wire and fife-hole probe measurements could now be compared with the computed uncertainties.

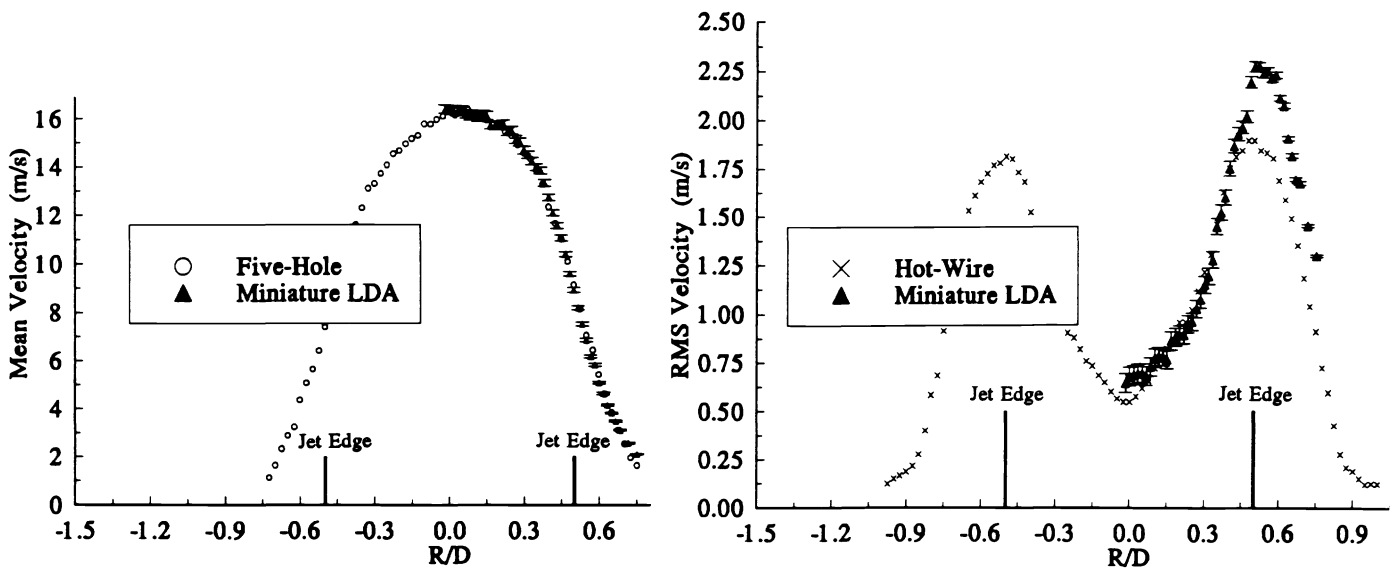

FIGURE 7
Free Jet Facility Corrected Mean and RMS Turbulent Velocity Profiles
With Uncertainty Bands
x/D = 2, H/D = 8

5.5 Relative weighting of uncertainty errors

It is interesting to examine the relative weighting of the uncertainty errors with respect to the mean velocity ($\bar{U}$) and the RMS turbulent velocity (u_{RMS}). Figure 8 displays a pie graph showing the relative weighting of the six uncertainty sources on the mean velocity and RMS turbulence measurements.

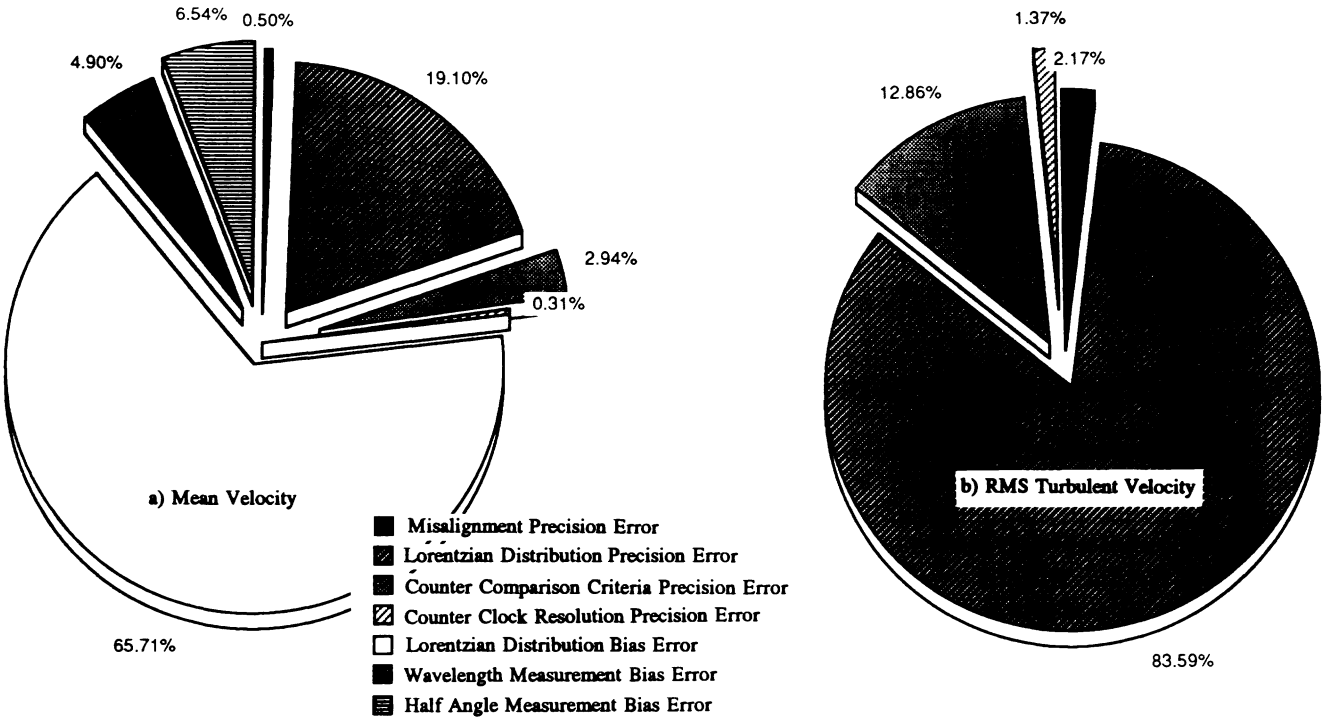

FIGURE 8
Relative Weighting of the Uncertainty Sources

6. SUMMARY AND CONCLUSIONS

It was desired to construct an accurate miniature solid state laser Doppler anemometer. To this end, the performance of an index guided laser diode in such a miniature LDA system was evaluated.

An intensive theoretical evaluation preceded hardware development. Laser diode technology was researched in an effort to reveal any possible complications with their use in an LDA system. Many problems were uncovered including; high beam divergence, high astigmatism, low coherence, multiple simultaneously emitted modes, elliptic beam profile, non-Gaussian intensity profile, and wavelength instabilities. Effective corrective measures were needed to counter each of the individual problems. The expected probe volume generated by laser diode beams was determined through an electrical field model and pseudo-Gaussian beam optics. It was found the probe volume had essentially the same dimensions as predicted through standard LDA theory, but the shape was much distorted. The distorted probe volume shape combined with the high wavefront curvatures associated with Lorentzian distributions was found to generate serious (+10%) frequency broadening through interference fringe gradients.

A thorough quantitative analysis was performed using experimental measurements. A stagnating round jet (Re = 30,000) was traversed with the miniature LDA ($\bar{U}$ and u_{RMS}), a five-hole probe ($\bar{U}$), and a single sensor hot-wire probe ($u_{eff,RMS}$). Following corrections for correctable LDA bias errors, measurement uncertainties were computed. The corrected measurements were compared to the five-hole and hot-wire probe measurements. Differences between the three measurement systems were evaluated taking into account the uncertainty bands of the miniature LDA data. The miniature LDA was found to produce accurate measurements of flow velocities. For the present LDA configuration the mean velocity measurements were accurate to 2% and the RMS turbulent velocity measurements were accurate to 5-20%. In most cases the predicted uncertainty was large enough to explain the error observed. The main source of uncertainty was found to be associated with the Lorentzian distribution in the crossing plane (x-z plane). It is recommended that future systems be constructed with the Gaussian profile in the crossing plane (x-z plane). This can easily be accomplished by rotating the laser diode and using appropriate 1/2 retarder wave plates for polarization control.

REFERENCES

Abernethy R. B., Benedict R. P., Dowdell R. B., "*ASME Measurement Uncertainty*," Journal of Fluids Engineering, Vol 107, June (1985).

Bopp S., Durst F., Müller R., Naqwi A., Tropea C., and Weber H., "*Small Laser-Doppler Anemometers Using Semiconductor Lasers and Avalanche Photodiodes*," Applications of Laser Anemometry to Fluid Mechanics, Fourth International Symposium, Springer-Verlag (1988).

Buus J., Single Frequency Semiconductor Lasers, The International Society for Optical Engineering pp. 1-5 (1991).

Damp S., "*Battery-Driven Miniature LDA-System With Semiconductor Laser Diode*," Applications of Laser Anemometry to Fluid Mechanics, Fourth International Symposium, Springer-Verlag (1988).

Durrani T. S., "*Frequency Domain Analysis*," Laser Systems in Flow Measurement, Plenum Press, Ch. 3, pp. 159-160 (1977).

Durst F., and Stevenson W. H., "*Influence of Gaussian Beam Properties on Laser Doppler Signals*," Applied Optics, Vol. 18, No. 4 (1979)

Durst F., Müller R., Naqwi A., "*Semiconductor Laser Doppler Anemometer for Applications in Aerodynamic Research*," AIAA Journal, Vol. 30, No. 4 (1991).

Hanson S., "*Broadening of the Measured Frequency Spectrum in a Differential Laser Anemometer Due to Interference Plane Gradients*," Journal of Physics D: Applied Physics, Vol 6 (1973).

Jentink H. W., van Beurden J. A. J., Helsdingen M. A., de Mul F. F. M., Suichies H. E., Aarnoudse J. G., and Greve J., "*A Compact Differential Laser Doppler Velocimeter Using a Semiconductor Laser*," IOP, (1987).

Naqwi A., Durst F., "*Focusing of Diode Laser Beams: a Simple Mathematical Model*," Applied Optics, Vol. 29, No. 12, April (1990).